Dalton Transactions

ROYAL SOCIETY OF CHEMISTRY

PAPER

View Article Online
View Journal | View Issue

Cite this: *Dalton Trans.*, 2026, **55**, 3703

Bicarbonate anion coordination assisted CO_2 capture by using urea–morpholine hybrid receptors in water

Zhiwen Sun, Ji Wang, Qingling Nie, Na Li, Zhihua Liu, Xiao-Juan Yang, Wei Zhao * and Biao Wu

Received 21st December 2025,
Accepted 30th January 2026

DOI: 10.1039/d5dt03056k

rsc.li/dalton

The development of energy-efficient sorbents for aqueous CO_2 capture remains a significant challenge. This work presents a new design strategy by integrating a tertiary amine (morpholine) with a urea motif into a single molecular receptor. This structure enables autonomous, base-free CO_2 capture in water, where the urea groups provide complementary hydrogen-bonding sites for (bi)carbonate anions, while the morpholine moiety acts as an internal proton acceptor. The resulting receptors demonstrate a rapid uptake of CO_2 from a simulated flue gas (10% CO_2/N_2), achieving a capacity of up to 1.22 mmol g^{-1}. Spectroscopic studies (NMR, MS) and structural analysis of a model complex confirm that the capture proceeds *via* hydrogen-bond-stabilized bicarbonate formation. Crucially, the captured CO_2 can be completely released under remarkably mild conditions, either by heating at *ca.* 40 °C or by simple N_2 purging at ambient temperature. The receptors exhibit excellent recyclability over multiple capture–release cycles without capacity loss. This study highlights the potential of fine-tuning supramolecular interactions—particularly hydrogen bonding combined with a built-in base—to create low-energy, water-compatible CO_2 capture systems.

Introduction

Effective capture of carbon dioxide (CO_2) is crucial for mitigating climate change, driving the search for materials that combine high adsorption capacity with low regeneration energy.[1–4] Conventional chemisorbents, such as inorganic bases, organic amines, and their polymeric or framework derivatives, typically rely on forming strong chemical bonds (*e.g.*, carbonates or carbamates).[5–17] While effective for capture, this strong binding often necessitates substantial energy input for CO_2 release. The challenge is further amplified in the presence of water, a ubiquitous component in flue gas and direct air capture streams. In aqueous environments, CO_2 hydration readily forms carbonic acid (H_2CO_3), and the interaction between organic amines and CO_2 tends to yield (bi) carbonate salts, instead of carbamate.[18] Consequently, achieving both high capture efficiency and energy-favorable desorption in water-rich media remains a significant scientific and technological challenge.

Hydrogen bonding has emerged as a key secondary interaction to regulate the properties of CO_2 capture and release. This is exemplified by strategic modifications in organic amine systems. Introducing intramolecular hydrogen-bond donors or acceptors, such as pyridine or amide groups adjacent to the reactive amines,[19–22] can stabilize CO_2 adducts (*e.g.*, carbamate or carbamic acid) through internal hydrogen bonding.[23–26] Such stabilization not only modulates binding strength but can also lower the regeneration energy by shifting the acid/zwitterion equilibrium toward more readily released neutral species, as demonstrated in aminopyridine solvents.[27] In these systems, the intramolecular hydrogen-bonding network is a critical descriptor for achieving low viscosity and reduced regeneration temperatures (as low as 60–80 °C).[28,29] Similarly, in diamide–diamine macrocycles, the carbamate product is encapsulated and stabilized by a multiple hydrogen bonding network.[30] In aqueous media, the design principle shifts toward employing strong, charge-assisted hydrogen bonds to capture these anions.[31–33] A seminal advance in this direction is the work by Custelcean *et al.* on bis-iminoguanidinium compounds.[34] The rigid, planar guanidine units protonate readily to form guanidinium cations that engage in complementary, strong hydrogen bonds with carbonate or bicarbonate anions, driving the spontaneous crystallization of insoluble frameworks from water and thereby removing CO_2 from the

Key Laboratory of Medicinal Molecule Science and Pharmaceutics Engineering of Ministry of Industry and Information Technology, School of Chemistry and Chemical Engineering, Beijing Institute of Technology, Beijing 102488, China.
E-mail: zhaochem@bit.edu.cn

air. Notably, regeneration of these sorbents, achieved by mild heating of the solid carbonate crystals to release CO_2, can occur at temperatures of 80–120 °C, underscoring how engineered hydrogen-bonding networks can enable energy–efficient capture–release cycles.[34–37] Collectively, these studies highlight hydrogen bonding as a versatile and powerful design element for tailoring CO_2 capture materials.

Like guanidium units, urea motifs can also bind oxyanions like carbonate and bicarbonate *via* anion coordination (*i.e.*, hydrogen bonding), and therefore we sought to extend this supramolecular strategy with urea-based absorbents. While conventional oligourea receptors require exogenous strong bases (*e.g.*, tetraalkylammonium hydroxides or fluorides) to activate CO_2 fixation,[38–44] we hypothesize that integrating a tertiary amine moiety directly into an oligourea scaffold may enable autonomous, base–free capture in water. In this design, the urea groups provide precise hydrogen–bonding sites to stabilize *in situ* formed HCO_3^-/CO_3^{2-} ions, while the tertiary amine serves as an intramolecular proton acceptor,[45–47] offering additional electrostatic stabilization and facilitating the proton–transfer processes essential for both capture and subsequent release (Fig. 2a).

Guided by this rationale, we designed and synthesized a series of small molecules that combine morpholine (a cyclic tertiary amine, Fig. 1) with urea motifs. These morpholine–urea compounds were evaluated for CO_2 capture performance in water without any external organic base. Remarkably, they demonstrated rapid and efficient adsorption of CO_2 directly from water, achieving a capacity of up to 0.75 mol mol^{-1} (1.22 mmol g^{-1}) for receptor **2**. More importantly, the captured CO_2 could be rapidly released under heating at *ca.* 40 °C, highlighting the regulation effect of anion coordination.

Results and discussion

The designed receptors **1** and **2** were prepared in two steps from the starting material 4-(2-aminoethyl) morpholine

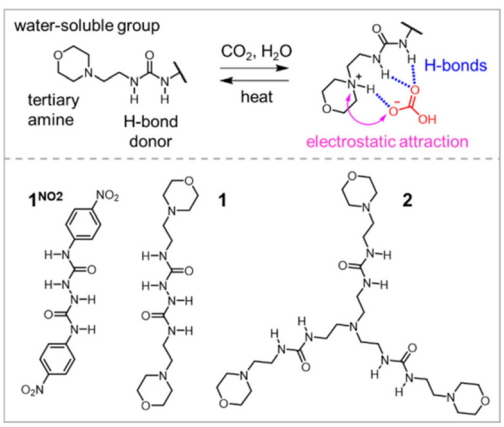

Fig. 1 Schematic illustration of the design principles of morpholine–urea receptors and their chemical structures.

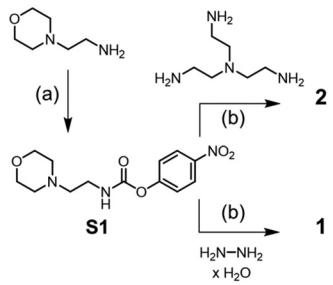

Scheme 1 Synthetic procedure of **1** and **2**. Conditions: (a) 4-nitrophenyl chloroformate, CH_2Cl_2, 0 °C, 80%; (b) dry CH_3CN, Et_3N, 50 °C, 72% for **1**, 81% for **2**.

(Scheme 1), with the overall yields of 58% and 65%, respectively. Both receptors can be easily synthesized on the gram scale, and their structures are characterized and confirmed by NMR and MS spectroscopy (Fig. S8–S16). These two receptors display good water solubility (up to 3 M), and the control receptor $\mathbf{1}^{\mathbf{NO2}}$ is not water soluble, which is directly synthesized from hydrazine hydrate and 4-nitrophenyl isocyanate (Fig. S1–S7).

The CO_2 capture performance of the two receptors was first evaluated in aqueous solution. A simulated flue gas (10% CO_2 in N_2) was bubbled at room temperature through 15 mL of a 20 mM aqueous solution of each receptor, while the uptake process was monitored in real time using a setup equipped with a high–precision CO_2 sensor (Fig. 2b). The initial pH of the receptor **1** solution was 8.96, consistent with the alkalinity provided by its morpholine group (pK_a ≈ 7.41 for *N*-methylmorpholine).[48,49] Upon CO_2 bubbling, the pH decreased to 6.77 for receptor **1** and to 6.99 for receptor **2**, confirming the existence of the HCO_3^- anion and H_2CO_3. As

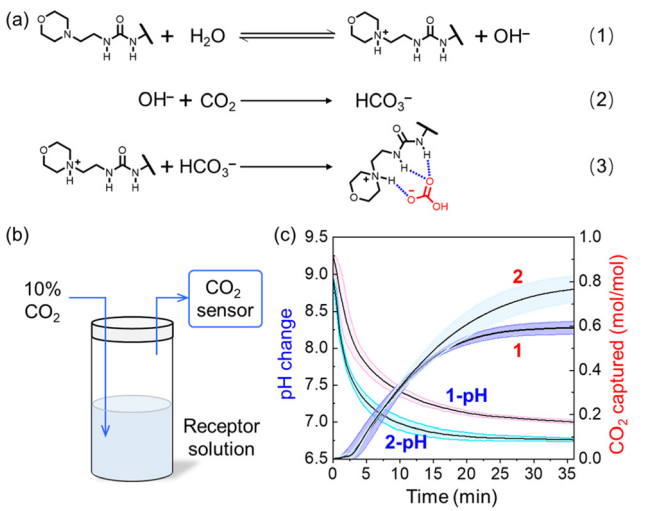

Fig. 2 (a) Mechanistic scheme of the formation of HCO_3^- and its binding with receptors in water. (b) A schematic diagram of the CO_2 capture experiment (gas input: 10% CO_2, 90% N_2; receptor solution: [receptor] = 20 mM, H_2O, room temperature). (c) The pH changes and the amount of CO_2 captured by using receptors **1** and **2**.

recorded by the CO_2 sensor, the amount of captured CO_2 increased gradually and reached a plateau within 30 minutes (Fig. S26–S28). The determined CO_2 capacity reached 0.75 mol of CO_2 per mole of receptor for **2** (0.75 mol per mol of receptor, equivalent to 1.22 mmol g^{-1}, Fig. 2c), which is higher than that of receptor **1** (0.58 mol mol^{-1}). This difference can be attributed to the higher number of urea and morpholine groups present in receptor **2**, which provide additional binding sites and basicity. The observed CO_2 uptake trends are consistent with the pH changes of the solutions. Notably, the absorption performance of both receptors is comparable to that of monoethanolamine (MEA), a benchmark industrial absorbent, which typically captures 0.4–0.5 mol of CO_2 per amine.[50–52] Nevertheless, these receptors are not suited for direct air capture applications, as their binding affinity is insufficient for the ultra-low CO_2 concentrations characteristic of ambient air (Fig. S30).

To elucidate the CO_2 capture mechanism, NMR and mass spectrometry (MS) experiments were performed. Following the completion of CO_2 uptake, as indicated by pH changes after *ca.* 30 min of CO_2 bubbling through a receptor-containing aqueous solution (20 mM), the resulting solutions were subjected to spectroscopic characterization.

As recorded in the ^{1}H NMR spectra, the urea NH signals (Ha and Hb) exhibited characteristic changes upon CO_2 capture. For receptor **1**, the original singlet at 6.78 ppm split into two doublets at 7.7 ppm and 6.8 ppm (Fig. 3a), whereas for receptor **2**, the signal shifted from 6.0 ppm to 6.2 ppm (Fig. 3b). These changes correspond to the hydrogen bonding between the urea groups and the HCO_3^- anion produced upon CO_2 absorption. Additionally, protons adjacent to the morpholinyl nitrogen (H2 and H3) in both receptors showed downfield shifts, consistent with the protonation of the tertiary amine and potential hydrogen bonding with the HCO_3^- anion. The ^{13}C NMR spectra further support the existence of the HCO_3^- anion. After CO_2 exposure, new peaks appeared at 160 ppm for **1** and 161 ppm for **2**, which are assigned to the HCO_3^- anion and consistent with reported data from the literature. Moreover, the carbonyl carbon atoms of the urea moieties exhibited clearly downfield shifts, with the most pronounced change observed for **1** ($\Delta\delta \approx 4$ ppm). These shifts reflect the electronic perturbation induced by HCO_3^- anion binding. In addition, the post-capture aqueous solutions of **1** and **2** were analysed by ESI-QTOF mass spectrometry. Distinct peaks were observed at 406.20 and 675.43, assigned to the adducts of $[\mathbf{1} + HCO_3]^-$ and $[\mathbf{2} + HCO_3]^-$, respectively (Fig. 3c), providing direct evidence for the formation of bicarbonate complexes. The MS results combined with NMR data to support the absorption of CO_2 as the HCO_3^- anion binding complexes with receptors.

To obtain structural insights into the CO_2 capture process, crystallization trials were conducted. Due to the high-water solubility of receptors **1** and **2**, single crystals of their HCO_3^- complexes could not be obtained. Instead, a control receptor $\mathbf{1}^{NO2}$, which bears terminal nitrophenyl groups and retains the bis(urea) hydrogen–bonding motif but exhibits lower water solubility, was employed. Slow vapor diffusion from acetonitrile/diethyl ether yielded single crystals of its HCO_3^- and CO_3^{2-} complexes (as tetramethylammonium salts) suitable for X–ray diffraction analysis (Fig. 4).

As shown in Fig. 4a, the HCO_3^- complex crystallizes in the space group *C*2/*c*, while the CO_3^{2-} complex crystallizes in the *C*2/*m* space group. Both structures display one–dimensional arrangements (along the *c*-axis or *b*-axis) stabilized by hydrogen bonds between the anions and the bis(urea) receptors. In

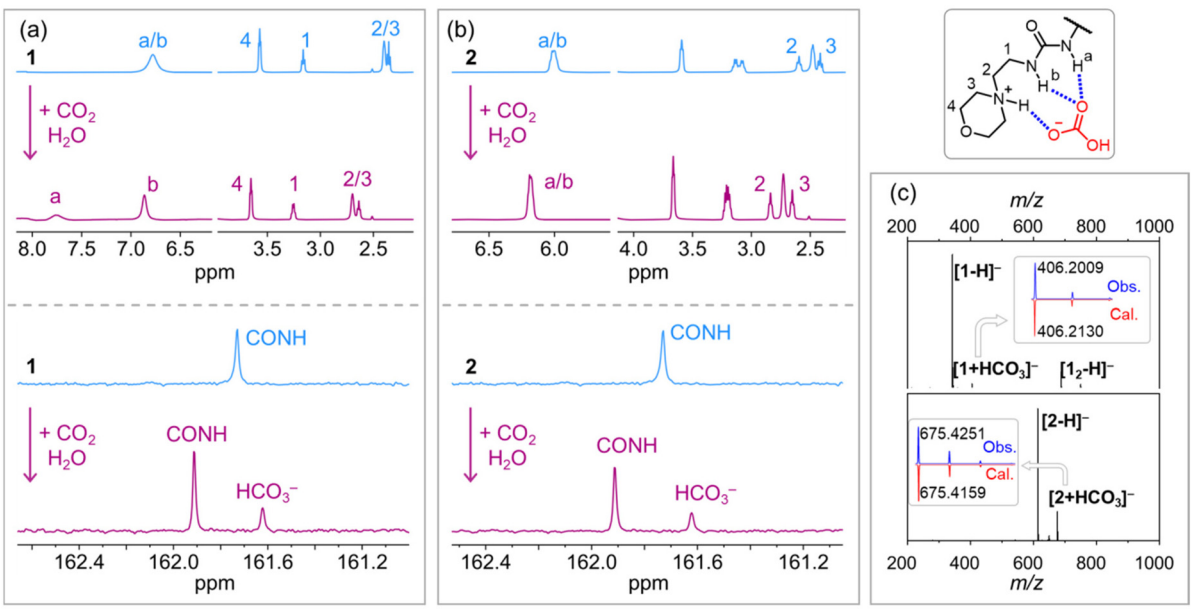

Fig. 3 ^{1}H and ^{13}C NMR spectra of receptors (a) **1** and (b) **2** before and after CO_2 capture (10% DMSO-d_6/90% H_2O, 298 K). (c) ESI-QTOF spectra of receptors after CO_2 capture, indicating the formation of HCO_3^- binding complexes.

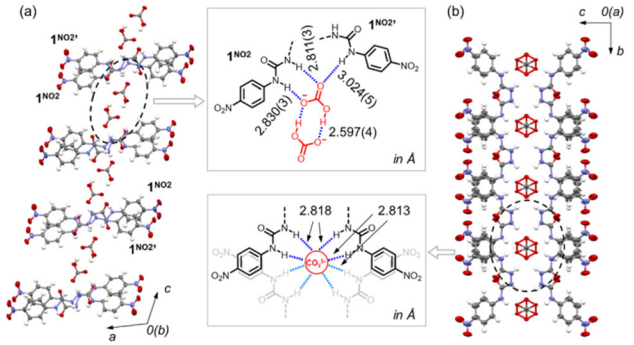

Fig. 4 Single crystal X-ray diffraction structures of (a) HCO_3^- and (b) CO_3^{2-} binding complexes of receptor $\mathbf{1}^{NO2}$. Solvent molecules and tetramethylammonium cations (TMA^+) are omitted for clarity. Their anion binding structures with urea units are shown in the middle boxes. The HCO_3^- anion dimerizes through two complementary hydrogen bonds and interacts with urea units through three hydrogen bonds. The CO_3^{2-} anion is disordered and stabilized by eight hydrogen bonds with four urea units.

the HCO_3^- complex, a 2 : 2 stoichiometry between the anion and $\mathbf{1}^{NO2}$ is observed. Every two HCO_3^- anions dimerize through two O–H···O hydrogen bonds (d = 2.597 Å), a recurring motif also reported in oligourea and guanidinium–based CO_2 capture systems. Such anti-electrostatic hydrogen bonding is also widely seen for hydroxy anion dimers in the solid state.[39,53–55] Each bicarbonate anion is further stabilized by three N–H···O hydrogen bonds from urea groups. Every two receptors adopt a parallel arrangement with an essentially linear conformation (Fig. S6).

In contrast, the CO_3^{2-} complex features a V–shaped receptor conformation. Each carbonate anion is engaged in eight N–H···O hydrogen bonds involving four different receptor molecules (Fig. 4b). The average N–H···O distance in the CO_3^{2-} complex (2.82 ± 0.01 Å) is notably shorter than that in the HCO_3^- analogue (2.89 ± 0.10 Å), reflecting stronger binding to carbonate. Along the b-axis, adjacent CO_3^{2-} ions are linked by urea groups from different receptors, forming an infinite one–dimensional hydrogen–bonded chain that extends into a rod–like framework structure (Fig. S7).

In contrast to receptors **1** and **2**, the control receptor $\mathbf{1}^{NO2}$ captures CO_2 only in the presence of an external base, such as fluoride or tetramethylammonium hydroxide (TMAOH), in acetonitrile or DMSO. This requirement is attributed to the absence of the built–in morpholine group, a feature that enables autonomous proton capture in **1** and **2**, and aligns with the behavior of other oligourea receptors reported earlier. Interestingly, once CO_2 is captured, the resulting HCO_3^- complex of $\mathbf{1}^{NO2}$ precipitates rapidly from acetonitrile solution within minutes, forming a hydrogen–bond–supported framework as seen in the solid state (Fig. 4). Such fast precipitation, commonly observed with guanidinium–based receptors, is seldom reported for urea–based systems. Furthermore, in the presence of TMA^+ as the countercation, the absorbed HCO_3^- anion cannot be thermally released as CO_2 gas (Fig. S17–S25). Reversible CO_2 release occurs only when free protons (H^+) are available in solution,[56] underscoring the crucial role of proton transfer in the regeneration step.

In the presence of TMA^+ as the countercation, the absorbed HCO_3^- anion cannot be thermally released as CO_2. This is because thermal regeneration of the absorbent necessitates the complete protonation of absorbed HCO_3^- to form labile carbonic acid (H_2CO_3), which then dissociates to release CO_2. Nevertheless, during the heating of $TMAHCO_3$ complexes, no labile protons are available for combination with HCO_3^-, thus precluding CO_2 release and absorbent regeneration. In contrast, the receptor utilized in our work allows the absorbed CO_2 to be converted into H^+ and HCO_3^- during the absorption process. Specifically, the generated H^+ resides on the protonated morpholine moieties, whereas HCO_3^- is connected to the urea groups *via* weak hydrogen bonds, constructing a fragile hydrogen-bonding network. This structural characteristic facilitates proton transfer from the protonated morpholine groups to HCO_3^- upon heating, which in turn promotes the formation of labile H_2CO_3 (Fig. 5a).

For receptors **1** and **2**, the captured CO_2 (in the form of HCO_3^-) can be readily released under mild heating, as initially demonstrated by variable–temperature ^{1}H NMR experiments. A solution of receptor **1** after CO_2 bubbling (10 mM, 10% DMSO-d_6/90% H_2O) was examined while increasing the temperature from 298 K to 308 K (35 °C). Upon heating, the urea NH signal (Ha) gradually disappeared, while the adjacent proton Hb showed a clear upfield shift (Fig. 5b). At 318 K (45 °C), the spectrum closely resembled that of the free receptor, indicating complete release of the HCO_3^- anion. A similar trend was observed for the receptor **2**. The recovery of the ^{1}H NMR signals corresponding to the free receptors confirms that hydrogen–bonding interactions with bicarbonate are effectively disrupted upon heating, resulting in the release of CO_2 gas. Such low–temperature CO_2 release is rarely reported, suggesting that hydrogen–bonding interaction can serve as a tunable tool for regulating both capture and release processes.

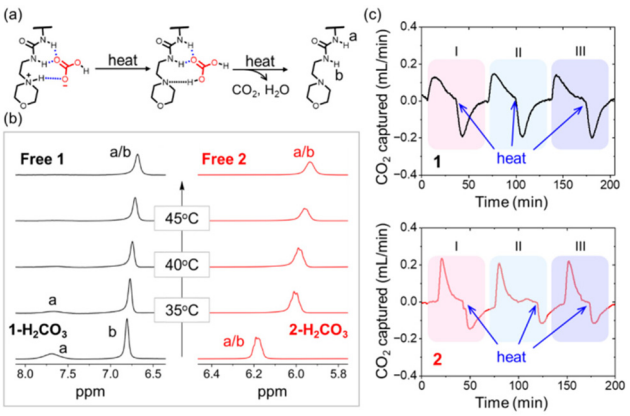

Fig. 5 (a) A schematic representation of the mechanism of CO_2 release. (b) Variable temperature ^{1}H NMR spectra of CO_2-binding receptors (10 mM, 10% DMSO-d_6/90% H_2O, 400 MHz). (c) Reversible CO_2 capture and release (upon heating at 40 °C).

To assess the recyclability of the receptors, reversible CO_2 capture and thermal release were monitored in real time using the CO_2 sensor setup (Fig. 2b). An aqueous solution of receptor **1** or **2** (20 mM, 15 mL) was continuously purged with 10% CO_2 in N_2. After uptake reached completion (~30 min), the solution was heated to 40 °C using a stir plate. The CO_2 sensor recorded a drop in outlet CO_2 concentration during the capture phase, followed by a return to the baseline level upon heating, which is consistent with the variable–temperature NMR results. This capture–release cycle was repeated multiple times without any loss in capacity (Fig. 5c), confirming excellent reversibility and stability of the receptors.

Furthermore, we found that CO_2 could also be liberated simply by purging the solution with pure N_2 gas (Fig. S31), a behavior similarly observed in other anion–based CO_2 capture systems where CO_2 is weakly bound. This result further underscores the low–energy character of CO_2 release in these urea–morpholine receptors. The integration of hydrogen–bonding motifs with a tertiary amine moiety enables effective capture while maintaining weak binding strength, thereby minimizing the energy penalty associated with regeneration, a feature attributed to the labile nature of the hydrogen–bonding network that stabilizes the bicarbonate anion.

Conclusions

In summary, we have designed and synthesized new urea–morpholine receptors capable of efficient and reversible CO_2 capture in water without adding external bases. The synergistic function of the urea hydrogen-bond donors and the tertiary amine proton acceptor facilitates direct CO_2 capture, forming stable bicarbonate complexes as verified by NMR, MS, and structural analysis using a crystalline model system. A key achievement is the exceptionally mild release of CO_2, achievable either by gentle heating (~40 °C) or inert gas purging, which underscores the low-energy penalty associated with disrupting the labile hydrogen-bonding network. The receptors maintain full capture capacity over multiple cycles, demonstrating robust recyclability. Compared to the control receptor $\mathbf{1}^{NO2}$, which requires added base and exhibits irreversible binding, the integrated morpholine design is essential for autonomous proton management and energy-efficient regeneration. This work establishes hydrogen-bonding donor/acceptor integration as a powerful supramolecular strategy for developing new, energy-lean carbon capture materials operable under practical, moisture-rich conditions.

Author contributions

Data curation, investigation and methodology: Z. Sun, J. Wang, Q. Nie, N. Li, and Z. Liu. Project administration, supervision and funding acquisition: W. Zhao, X.-J. Yang, and B. Wu. Conceptualization and writing (original draft, reviewing & editing): W. Zhao and Z. Sun.

Conflicts of interest

There are no conflicts to declare.

Data availability

Data supporting this article have been included as part of the supplementary information (SI). Supplementary information: details of syntheses, single crystal structures and NMR results. See DOI: https://doi.org/10.1039/d5dt03056k.

CCDC 2516702 (carbonate complex), 2516703 (bicarbonate complex), 2517602 (receptor $\mathbf{1}^{NO2}$) and 2517603 (receptor **1**) contain the supplementary crystallographic data for this paper.[57a–d]

Acknowledgements

This work was supported by the National Natural Science Foundation of China (22101024) and the Beijing Municipal Natural Science Foundation (2222025). We thank Prof. Zheng Meng for helpful discussions and the setup of the CO_2 absorption equipment. We are also thankful for the support from the Analysis & Testing Center of Beijing Institute of Technology for data collection.

References

1 D. S. Sholl and R. P. Lively, *Nature*, 2016, **532**, 435–437.
2 D. M. Reiner, *Nat. Energy*, 2016, **1**, 15011.
3 K. S. Lackner, *Science*, 2003, **300**, 1677–1678.
4 S. Y. W. Chai, L. H. Ngu and B. S. How, *Greenhouse Gases: Sci. Technol.*, 2022, **12**, 394–427.
5 E. S. Sanz-Pérez, C. R. Murdock, S. A. Didas and C. W. Jones, *Chem. Rev.*, 2016, **116**, 11840–11876.
6 H. Adun, J. D. Ampah, O. Bamisile and Y. Hu, *Sustain. Prod. Consum.*, 2024, **45**, 386–407.
7 A. Deprez, P. Leadley, K. Dooley, P. Williamson, W. Cramer, J.-P. Gattuso, A. Rankovic, E. L. Carlson and F. Creutzig, *Science*, 2024, **383**, 484–486.
8 S. A. Didas, S. Choi, W. Chaikittisilp and C. W. Jones, *Acc. Chem. Res.*, 2015, **48**, 2680–2687.
9 F. Inagaki, C. Matsumoto, T. Iwata and C. Mukai, *J. Am. Chem. Soc.*, 2017, **139**, 4639–4642.
10 F. A. Chowdhury, H. Yamada, T. Higashii, K. Goto and M. Onoda, *Ind. Eng. Chem. Res.*, 2013, **52**, 8323–8331.
11 C. Perinu, I. M. Bernhardsen, D. D. D. Pinto, H. K. Knuutila and K.-J. Jens, *Ind. Eng. Chem. Res.*, 2018, **57**, 1337–1349.
12 X. Li, X. Zhao, Y. Liu, T. A. Hatton and Y. Liu, *Nat. Energy*, 2022, **7**, 1065–1075.
13 J. Liu, M. Yang, X. Zhou and Z. Meng, *J. Am. Chem. Soc.*, 2024, **146**, 33093–33103.
14 J. Singh, H. Bhunia and S. Basu, *J. Environ. Manage.*, 2019, **250**, 109457.

15 F. Zhao, B. Zhu, L. Wang and J. Yu, *J. Colloid Interface Sci.*, 2024, **659**, 486–494.
16 H. Li, M. E. Zick, T. Trisukhon, M. Signorile, X. Liu, H. Eastmond, S. Sharma, T. L. Spreng, J. Taylor, J. W. Gittins, C. Farrow, S. A. Lim, V. Crocellà, P. J. Milner and A. C. Forse, *Nature*, 2024, **630**, 654–659.
17 Y. Yu, Y. Shen, X. Zhou, F. Liu, S. Zhang, S. Lu, J. Ye, S. Li, J. Chen and W. Li, *Chem. Eng. J.*, 2022, **428**, 131241.
18 J. K. Stolaroff, D. W. Keith and G. V. Lowry, *Environ. Sci. Technol.*, 2008, **42**, 2728–2735.
19 J. N. Gayton, Q. Li, L. Sanders, R. R. Rodrigues, G. Hill and J. H. Delcamp, *ACS Omega*, 2020, **5**, 11687–11694.
20 A. F. Eftaiha, A. K. Qaroush, B. O. Al-Shami and K. I. Assaf, *Org. Biomol. Chem.*, 2021, **19**, 3873–3881.
21 D. Wei, R. Sang, A. Moazezbarabadi, H. Junge and M. Beller, *JACS Au*, 2022, **2**, 1020–1031.
22 A. Li, Y. Liu, K. Luo and Q. He, *CCS Chem.*, 2024, **6**, 2882–2894.
23 J. S. Derrick, M. Loipersberger, S. K. Nistanaki, A. V. Rothweiler, M. Head-Gordon, E. M. Nichols and C. J. Chang, *J. Am. Chem. Soc.*, 2022, **144**, 11656–11663.
24 G. Manca, F. Barzagli, J. Nagy, M. Munzarová, M. Peruzzini and A. Ienco, *Fuel*, 2024, **378**, 132859.
25 M. Ma, Y. Liu, Y. Chen, G. Jing, B. Lv, Z. Zhou and S. Zhang, *J. CO2 Util.*, 2023, **67**, 102277.
26 S. Meng, T. H. Lambert and P. J. Milner, *J. Am. Chem. Soc.*, 2025, **147**, 6786–6794.
27 D. Malhotra, D. C. Cantu, P. K. Koech, D. J. Heldebrant, A. Karkamkar, F. Zheng, M. D. Bearden, R. Rousseau and V.-A. Glezakou, *ACS Sustainable Chem. Eng.*, 2019, **7**, 7535–7542.
28 M. K. Leszczynski, D. Kornacki, M. Terlecki, I. Justyniak, G. I. Miletic, I. Halasz, P. Bernatowicz, V. Szejko and J. Lewinski, *ACS Sustainable Chem. Eng.*, 2022, **10**, 4374–4380.
29 A. J. Huang, A. K. Gupta, H. Z. H. Jiang, H. Zhuang, M. B. Wenny, R. A. Klein, H. Kwon, K. R. Meihaus, H. Furukawa, C. M. Brown, J. A. Reimer, W. A. de Jong and J. R. Long, *J. Am. Chem. Soc.*, 2025, **147**, 10519–10529.
30 Q. Q. Wang, V. W. Day and K. Bowman-James, *Org. Lett.*, 2014, **16**, 3982–3985.
31 S. Pawlędzio and X. Wang, *Crystals*, 2024, **14**, 77–103.
32 H. Cai, X. Zhang, L. Lei and C. Xiao, *ACS Omega*, 2020, **5**, 20428–20437.
33 G. Mezei, *Chem*, 2019, **5**, 499–501.
34 C. A. Seipp, N. J. Williams, M. K. Kidder and R. Custelcean, *Angew. Chem., Int. Ed.*, 2017, **56**, 1042–1045.
35 U. I. Premadasa, V. Bocharova, A. R. Miles, D. Stamberga, S. Belony, V. S. Bryantsev, A. Elgattar, Y. Liao, J. T. Damron, M. K. Kidder, B. Doughty, R. Custelcean and Y. Z. Ma, *Angew. Chem., Int. Ed.*, 2023, **62**, e202304957.
36 F. M. Brethomé, N. J. Williams, C. A. Seipp, M. K. Kidder and R. Custelcean, *Nat. Energy*, 2018, **3**, 553–559.
37 N. J. Williams, C. A. Seipp, F. M. Brethomé, Y.-Z. Ma, A. S. Ivanov, V. S. Bryantsev, M. K. Kidder, H. J. Martin, E. Holguin, K. A. Garrabrant and R. Custelcean, *Chem*, 2019, **5**, 719–730.
38 A. Pramanik, M. E. Khansari, D. R. Powell, F. R. Fronczek and M. A. Hossain, *Org. Lett.*, 2014, **16**, 366–369.
39 U. Manna and G. Das, *CrystEngComm*, 2019, **21**, 65–76.
40 I. Ravikumar and P. Ghosh, *Chem. Commun.*, 2010, **46**, 1082–1084.
41 R. Chutia and G. Das, *Dalton Trans.*, 2014, **43**, 15628–15637.
42 R. Dutta, S. Chakraborty, P. Bose and P. Ghosh, *Eur. J. Inorg. Chem.*, 2014, **2014**, 4134–4143.
43 U. Manna and G. Das, *CrystEngComm*, 2018, **20**, 3741–3754.
44 S. Kayal, U. Manna and G. Das, *Inorg. Chim. Acta*, 2019, **486**, 576–581.
45 G. Gao, B. Xu, X. Gao, W. Jiang, Z. Zhao, X. Li, C. Luo, F. Wu and L. Zhang, *Chem. Eng. J.*, 2023, **473**, 145277.
46 X. Li, J. Hou, H. Sui, L. Sun and L. Xu, *Materials*, 2018, **11**, 2431.
47 X. Zhou, D. Wang, C. Liu, G. Jing, B. Lv and D. Wang, *J. Environ. Sci.*, 2024, **140**, 146–156.
48 C. Yu, H. Ling, Z. Shen, H. Yang, D. Cao and X. Hu, *AlChE J.*, 2024, **70**, e18551.
49 K. Liu, K. M. Jinka, J. E. Remias and K. Liu, *Ind. Eng. Chem. Res.*, 2013, **52**, 15932–15938.
50 J. I. Huertas, M. D. Gomez, N. Giraldo and J. Garzón, *J. Chem.*, 2015, 965015.
51 M. Abdi-Khanghah, F. Hadavimoghaddam, S. Atashrouz, E. Nasirzadeh, M. A. Abuswer, M. Ostadhassan, A. Mohaddespour and A. Hemmati-Sarapardeh, *Digit. Chem. Eng.*, 2025, **15**, 100235.
52 M. N. Procopio, G. Urquiza, L. Castro and V. Zezatti, *Results Eng.*, 2023, **19**, 101286.
53 U. Manna, S. Kayal, B. Nayak and G. Das, *Dalton Trans.*, 2017, **46**, 11956–11969.
54 M. Giri and T. Guchhait, *ChemPlusChem*, 2024, **89**, e202400405.
55 U. Manna, S. Kayal, S. Samanta and G. Das, *Dalton Trans.*, 2017, **46**, 10374–10386.
56 B. Lv, B. Guo, Z. Zhou and G. Jing, *Environ. Sci. Technol.*, 2015, **49**, 10728–10735.
57 (*a*) CCDC 2516702: Experimental Crystal Structure Determination, 2026, DOI: 10.5517/ccdc.csd.cc2qgtyz; (*b*) CCDC 2516703: Experimental Crystal Structure Determination, 2026, DOI: 10.5517/ccdc.csd.cc2qgtz0; (*c*) CCDC 2517602: Experimental Crystal Structure Determination, 2026, DOI: 10.5517/ccdc.csd.cc2qhrzz; (*d*) CCDC 2517603: Experimental Crystal Structure Determination, 2026, DOI: 10.5517/ccdc.csd.cc2qhs01.